





# Improving the XRani Distribution's Inference: Applying Confidence Intervals to PM2.5 Concentration Data Collected in Bangkok, Thailand



Wararit Panichkitkosolkul<sup>1,2,\*</sup>, Wichai Witayakiattilerd<sup>1,2</sup>

<sup>1</sup> Department of Mathematics and Statistics, Faculty of Science and Technology, Thammasat University, Pathum Thani, 12120, Thailand

E-mails: wararit@mathstat.sci.tu.ac.th

<sup>2</sup> Thammasat University Research Unit in Mathematical Sciences and Applications, Pathum Thani, 12120,

Thailand

E-mails: wichai@mathstat.sci.tu.ac.th

\*Corresponding author.

Received: 30 April 2025 / Accepted: 5 September 2025

Abstract This paper developed and assessed four methods for constructing confidence intervals (CIs) for the parameter of the XRani distribution, which is frequently applied in the analysis of lifetime data. The CIs examined include the likelihood-based CI, Wald-type CI, bootstrap-t CI, and the bias-corrected and accelerated (BCa) bootstrap CI. To evaluate their performance, both a simulation study and a real-world application were conducted. The evaluation criteria focused on empirical coverage probability (ECP) and average width (AW) across a range of scenarios. To enhance computational efficiency, an explicit analytical expression for the Wald-type CI was derived. Simulation results demonstrated that the likelihood-based and Wald-type CIs consistently achieved ECPs close to the nominal 0.95 confidence level across most scenarios. In contrast, for smaller sample sizes, the bootstrap-t and BCa bootstrap methods yielded lower ECPs. However, as sample sizes increased, the ECPs of both bootstrap methods gradually approached the nominal level. The parameter values were also found to influence performance: at lower parameter values, all CIs performed well, with the likelihood-based and Wald-type methods maintaining an ECP close to 0.95. At higher parameter values and smaller sample sizes, however, the bootstrap-t and BCa methods exhibited diminished coverage probabilities. The practical utility of these CI methods was further demonstrated through the applications to PM2.5 concentration data collected in Bangkok, Thailand. The results from this empirical analysis corroborated the findings of the simulation study, thereby affirming the robustness and applicability of the proposed CI methods.

MSC: 62N02, 62F10, 62G09, 62P12

Keywords: lifetime distribution; interval estimation; likelihood function; Wald; bootstrap

Published online: 21 September 2025 © 2025 By TaCS-CoE, All rights reserve.



Published by Center of Excellence in Theoretical and Computational Science (TaCS-CoE)

Please cite this article as: W. Panichkitkosolkul et al., Improving the XRani Distribution's Inference: Applying Confidence Intervals to PM2.5 Concentration Data Collected in Bangkok, Thailand, Bangmod Int. J. Math. & Comp. Sci., Vol. 11 (2025), 377–409. https://doi.org/10.58715/bangmodjmcs.2025.11.17

## 1. Introduction

Lifetime data analysis is a statistical approach used to estimate the time until the occurrence of a specific event, such as system failure or the onset of a particular incident [1]. A distinguishing characteristic of this methodology is its ability to manage censored data, wherein some subjects do not experience the event of interest within the study period. This aspect necessitates the use of specialized statistical techniques designed to account for incomplete observations.

Lifetime data are typically non-normally distributed and are often modeled using probability distributions such as the Weibull, exponential, gamma, log-normal, or Lindley distributions. Among these, the exponential and Lindley distributions are frequently employed due to their mathematical simplicity and analytical tractability. However, both distributions exhibit significant limitations. The exponential distribution assumes a constant hazard rate and possesses a memoryless property [19], assumptions that often do not align with empirical data. Although the Lindley distribution provides a refinement over the exponential model [14], it still falls short in capturing the complexity of datasets characterized by non-constant hazard rates and heterogeneous failure time behaviors. Therefore, there is a compelling need for the development of novel and flexible probability distributions capable of more accurately modeling lifetime data. Such advancements would contribute to improved data fitting and more reliable inferential outcomes in survival and reliability analyses.

Researchers employ a variety of strategies to construct novel probability distributions or enhance the performance of existing classical models. A widely adopted technique involves the introduction of additional parameters to improve model flexibility. Examples include the two-parameter Lindley distribution [27], the three-parameter Lindley distribution [37], the exponentiated Shanker distribution [20], and the two-parameter Shanker distribution [22]. While these extensions offer greater adaptability in fitting diverse datasets, they also increase model complexity, potentially compromising interpretability.

This added complexity may result in overfitting, particularly when applied to small sample sizes, thereby necessitating larger datasets to obtain reliable estimates. Moreover, the estimation of parameters becomes more intricate, often requiring sophisticated numerical techniques. The computational burden associated with such models can pose challenges in practical applications, especially in resource-constrained environments.

In contrast to approaches that increase model complexity through the addition of parameters, several researchers have introduced new mixed probability distributions that achieve enhanced flexibility without the need for supplementary parameters. Notable examples include the Shanker distribution [28], the Aradhana distribution [30], the Rani distribution [34], the Gharaibeh distribution [13], the Iwueze distribution [10], the Juchez distribution [9], and the Ola distribution [2]. These mixed distributions, which are often derived as extensions or generalizations of the Lindley distribution, have demonstrated superior performance compared to classical models, particularly in terms of flexibility and goodness-of-fit. Their ability to accommodate a wide variety of data patterns makes them highly adaptable and valuable for practical applications across numerous fields. As such, they offer a robust and efficient framework for modeling lifetime and reliability data without the trade-offs associated with parameter-rich models.

Among the various recently proposed distributions, the XRani distribution, introduced by Etaga et al. [11], has emerged as a notable advancement. It is formulated as a mixture of the exponential and Rani distributions and has exhibited remarkable efficacy in modeling lifetime data. Empirical studies, including analyses of Vinyl chloride concentration data and monthly sulfur dioxide levels, have demonstrated the XRani distributions superior performance and robustness across a variety of environmental and reliability contexts.

Compared to classical lifetime distributions, the XRani distribution offers superior adaptability in modeling datasets with moderate to high kurtosis and non-monotonic hazard rate behaviorsituations where distributions such as the exponential, Weibull, or Lindley often fail to capture the underlying complexity. While recently developed one-parameter mixed distributions, including the Shanker, Aradhana, Gharaibeh, Iwueze, Juchez, and Ola distributions, have improved flexibility without introducing additional parameters, their performance may deteriorate when dealing with data that simultaneously exhibit skewness, heavy tails, and varying hazard shapes. The XRani distribution retains the analytical simplicity of one-parameter distributions while enhancing tail flexibility and accommodating diverse hazard rate forms. This unique balance between interpretability, robustness, and goodness-of-fit positions the XRani distribution as a practical and efficient alternative for lifetime data analysis in real-world settings, particularly when both distribution simplicity and fitting accuracy are essential. These characteristics motivate the present studys focus on inference procedures for the XRani distribution, particularly in applications where interpretability and fit are both essential.

The confidence interval (CI) is a fundamental statistical tool used to quantify the uncertainty associated with parameter estimation in the context of statistical inference. It provides a range of plausible values within which the true parameter is expected to lie with a specified level of confidence. Constructing accurate CIs is particularly critical in lifetime data analysis, where precise parameter estimation directly impacts model validity and the reliability of inferential conclusions.

Despite the growing interest in the XRani distribution and its demonstrated effectiveness in modeling complex lifetime datasets, a comprehensive review of the existing literature reveals a notable gap: no studies to date have developed or assessed confidence interval estimation methods specifically tailored for the XRani distribution. This absence represents a critical shortcoming, particularly given the distribution's increasing relevance in real-world applications.

To address this gap, the present study proposes four distinct methods for constructing confidence intervals for the XRani distribution's parameter. To the best of our knowledge, this is the first study to develop and assess the CI estimation methods for the XRani distribution. These include: the likelihood-based CI, the Wald-type CI, the bootstrapt CI, and the bias-corrected and accelerated (BCa) bootstrap CI. Each method offers unique advantages in terms of coverage accuracy, computational feasibility, and robustness to distributional assumptions. To systematically evaluate the performance of these four CI estimation techniques, extensive Monte Carlo simulation experiments were conducted under varying sample sizes and parameter settings.

In addition to simulation-based validation, the practical utility of the proposed approaches was demonstrated through an empirical application to real environmental data. Specifically, two datasets on PM2.5 concentrations in Bangkok were analyzed using the XRani distribution, with all four CI estimation methods applied to assess and compare their performance in real-world conditions.

This study makes several contributions to the statistical literature. First, it is the first to systematically investigate and compare interval estimation procedures for the XRani

distribution—a flexible one-parameter lifetime model capable of capturing skewed and heavy-tailed data patterns. Second, the study explores the performance of both classical and bootstrap-based CI methods, offering practical guidance for implementation. Lastly, by applying the XRani distribution to real PM2.5 datasets, this paper demonstrates the relevance of the proposed methods to environmental monitoring, bridging methodological development with real-world application.

The remainder of this paper is organized as follows. Section 2 introduces the Rani and the XRani distributions, point parameter estimation, and outlines the four methods for constructing CIs. Section 3 presents the simulation studies and results. Section 4 applies the proposed methods to two real-world PM2.5 datasets. Section 5 concludes with key findings. The practical recommendations, limitations, and directions for future work are provided in Sections 6, 7, and 8, respectively.

## 2. Methodology

This section provides an overview of the XRani distribution, with emphasis on point estimation of its parameter and the construction of CIs. The discussion includes the application of maximum likelihood estimation for obtaining the point estimate, as well as several approaches for constructing CIs to assess the precision and reliability of the estimated parameter.

#### 2.1. The Rani and the Xrani Distributions

The Rani distribution is derived as a mixture of the exponential and gamma distributions, with specific mixing probabilities applied to combine the two. In this formulation, the gamma distribution is defined with a rate parameter, denoted as  $\theta$ , and a shape parameter set to 5. Let X denote a random variable that follows the Rani distribution with parameter  $\theta$ . The probability density function (PDF) of the Rani distribution can be derived using a mixed model comprising two components, each weighted by their respective mixing probabilities, as follows:

$$f_{\text{Rani}}(x;\theta) = p \cdot f_{\text{Exp}}(x;\theta) + (1-p) \cdot f_{\text{Gam}}(x;\theta,5), \tag{2.1}$$

where  $f_{\rm Exp}(x;\theta)=\theta e^{-\theta x}$  is the PDF of the exponential distribution with rate  $\theta$  and  $f_{\rm Gam}(x;\theta,5)$  is the PDF of the gamma distribution with shape parameter 5 and rate parameter  $\theta$  and the mixing proportion is  $p=\theta^5/(\theta^5+24)$ . The PDF of the Rani distribution is expressed as follows:

$$f_{\text{Rani}}(x;\theta) = \frac{\theta^5}{\theta^5 + 24} (\theta + x^4) e^{-\theta x}, \quad x > 0, \ \theta > 0,$$

Figure 1 illustrates the pdf plot of the Rani distribution for various parameter values.

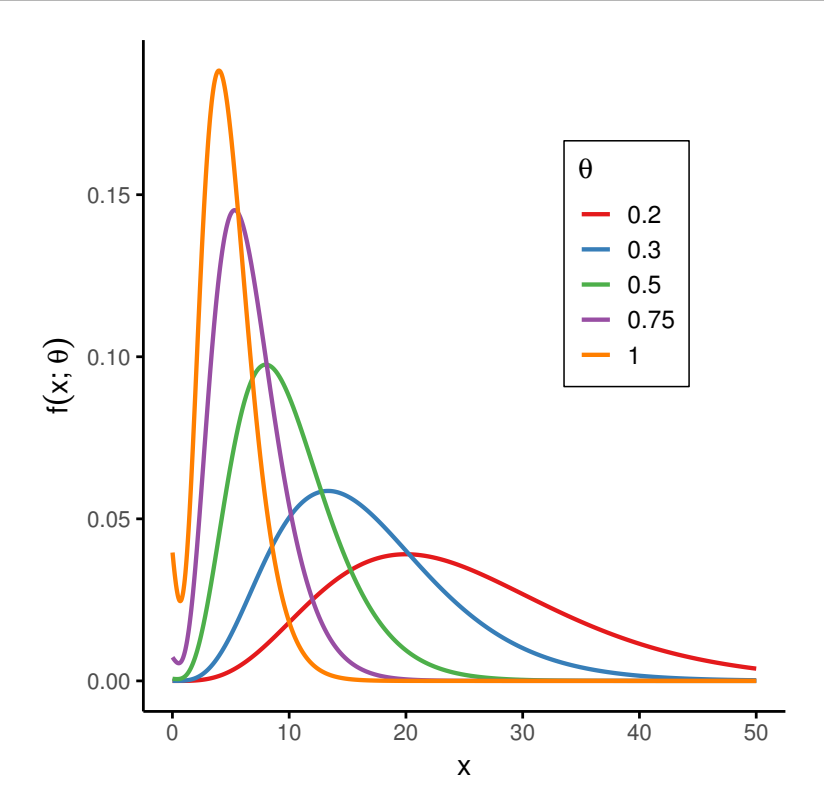


FIGURE 1. The PDF plot of the Rani distribution for different parameter settings.

Etaga et al. [11] introduced the XRani distribution, a one-parameter probability distribution developed as a more flexible extension of the Rani distribution. Let  $X \sim \text{XRani}(\theta)$ . The XRani distribution is defined as

$$f_{\mathrm{XRani}}(x;\theta) = p \cdot f_{\mathrm{Exp}}(x;\theta) + (1-p) \cdot f_{\mathrm{Rani}}(x;\theta),$$

where  $f_{\rm Exp}(x;\theta)=\theta e^{-\theta x}$  is the PDF of the exponential distribution with rate  $\theta$  and  $f_{\rm Rani}(x;\theta)$  is the PDF of the Rani distribution, given in Equation 2.1 and the mixing proportion is  $p=\theta^5/(\theta^5+24)$ . The PDF of the XRani distribution is mathematically defined in the equation below

$$f_{\text{XRani}}(x;\theta) = \frac{\theta^5}{(\theta^5 + 24)^2} (\theta^6 + 48\theta + 24x^4) e^{-\theta x}, \quad x > 0, \ \theta > 0.$$

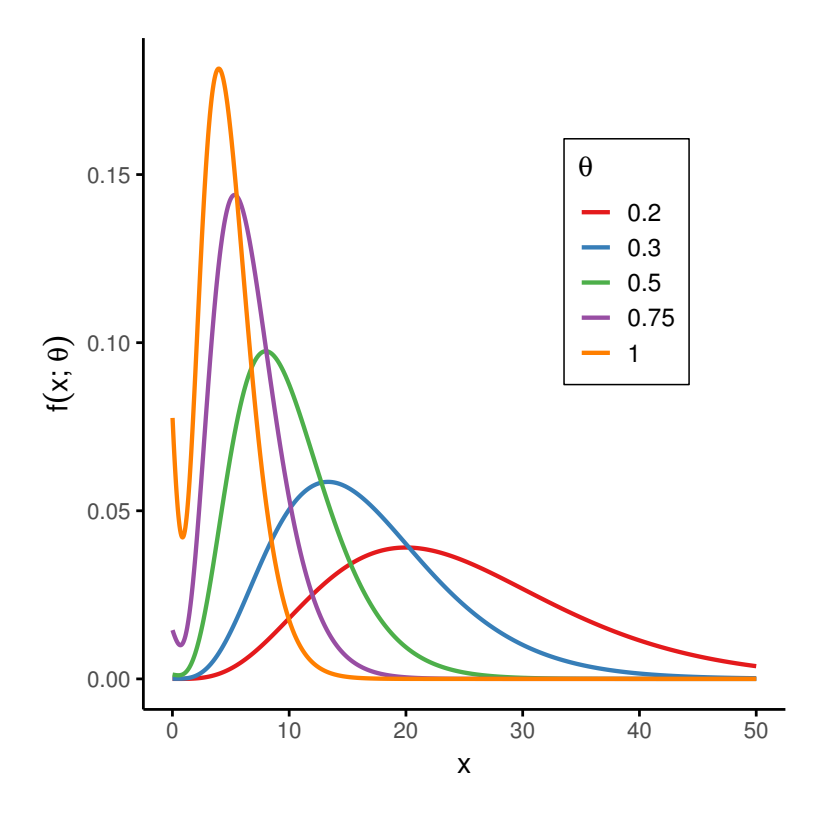


FIGURE 2. The PDF plot of the XRani distribution for different parameter settings.

Figures 1 and 2 demonstrate that the Rani and XRani distributions can take various shapes, including monotonic and unimodal forms. This one-parameter flexibility enables it to model skewed and heavy-tailed data effectively, making it a simple yet powerful tool for practical applications.

Some key statistical properties of the XRani distribution are outlined below, including the  $r^{\rm th}$  moment, mean, variance, survival function, and hazard function. The  $r^{\rm th}$  moment of a random variable X following the XRani distribution is given by

$$\mu'_r = E(X^r) = \frac{\theta^{-r} \left\{ 24(r+4)! + \theta^{r+10} + 480\theta^{r+5} \right\}}{(\theta^5 + 24)^2}; \quad r = 1, 2, \dots$$

The mean  $(\mu)$  and variance  $(\sigma^2)$  of the XRani distribution are given by

$$\mu = \frac{2880 + 48\theta^5 + \theta^{10}}{\theta \left(24 + \theta^5\right)^2},$$

and

$$\sigma^2 = \frac{17280 - 2880\theta + 96\theta^5 - 48\theta^6 + 2\theta^{10} - \theta^{11}}{\theta^2 (24 + \theta^5)^2}.$$



The skewness coefficient  $(\zeta)$ , kurtosis coefficient  $(\eta)$ , and coefficient of variation  $(\psi)$  of the XRani distribution are given as follows:

$$\zeta = \frac{6 \left(\theta^{10} + 48\theta^5 + 20160\right) \left(24 + \theta^5\right)^4}{\left(1658880 + 608256\theta^5 + 14976\theta^{10} + 96\theta^{15} + \theta^{20}\right)^{3/2}},$$

$$\eta = \frac{24 \left(24 + \theta^5\right)^6 \left(40320 + 48\theta^5 + \theta^{10}\right)}{\left(1658880 + \theta^5 \left(48 + \theta^5\right) \left(12672 + 48\theta^5 + \theta^{10}\right)\right)^2},$$

$$\psi = \frac{\sqrt{1658880 + 608256\theta^5 + 14976\theta^{10} + 960\theta^{15} + \theta^{20}}}{\left(24 + \theta^5\right)^2 \left(2880 + 48\theta^5 + \theta^{10}\right)}.$$

The survival and hazard rate functions are respectively

$$S(x) = \left\{ 1 + \frac{1}{(\theta^5 + 24)^2} \left[ 24\theta^4 x^4 + 960\theta^3 x^3 + 2880\theta^2 x^2 + 5760x \right] \right\} e^{-\theta x},$$

and

$$hrf(x) = \frac{\theta^{11} + 480\theta^6 + 240\theta^5 x^4}{\theta^{10} + 480\theta^5 + 576 + 240\theta^4 x^4 + 960\theta^3 x^3 + 2880\theta^2 x^2 + 5760x}.$$

Examining the structure of the XRani distribution reveals that it is a mixture of the exponential distribution and the Rani distribution, where the latter is itself a mixture of the exponential and gamma distributions with positive parameters. Consequently, the tail behavior of the XRani distribution exhibits the following property: as  $x \to \infty$ , the probability density decays exponentially, approximately as  $e^{-\theta x}$ . This exponential decay indicates that the XRani distribution is *light-tailed*, as all moments are finite. Therefore, the probability of observing extreme values is much lower compared to heavy-tailed distributions such as the Pareto or Cauchy.

#### 2.2. Point Parameter Estimation

The point estimator for the parameter of the XRani distribution can be derived using the maximum likelihood (ML) method. This approach involves constructing the likelihood function based on a given sample and then determining the parameter value that maximizes this function, as outlined in the following steps.

## Step 1: Find the likelihood function

The likelihood function  $L(\theta; x_i)$  represents the joint probability of observing a random sample drawn from the XRani distribution. It is defined as:

$$L(\theta; x_i) = \left(\frac{\theta^5}{(\theta^5 + 24)^2}\right)^n \cdot \prod_{i=1}^n (\theta^6 + 48\theta + 24x_i^4) \cdot e^{-\theta \sum_{i=1}^n x_i}.$$

#### Step 2: Find the log-likelihood function

Due to the mathematical complexity involved in directly differentiating the likelihood function, the log-likelihood function is employed to facilitate the differentiation process. The log-likelihood function is given by

$$\log L(\theta; x_i) = n \log \left( \frac{\theta^5}{(\theta^5 + 24)^2} \right) + \sum_{i=1}^n \log \left( \theta^6 + 48\theta + 24x_i^4 \right) - \theta \sum_{i=1}^n x_i.$$

#### Step 3: Differentiate the log-likelihood function

To determine the value of  $\theta$  that maximizes the log-likelihood function, the derivative of log  $L(\theta; x_i)$  with respect to  $\theta$  is computed. This yields the score function  $S(\theta; x_i)$ , which is expressed as follows:

$$S(\theta; x_i) = \frac{\partial}{\partial \theta} \log L(\theta; x_i)$$

$$= \frac{\partial}{\partial \theta} \left[ 5n \log(\theta) - 2n \log(\theta^5 + 24) + \sum_{i=1}^n \log(\theta^6 + 48\theta + 24x_i^4) - \theta \sum_{i=1}^n x_i \right]$$

$$= \frac{5n}{\theta} - \frac{10n\theta^4}{\theta^5 + 24} + \sum_{i=1}^n \frac{6\theta^5 + 48}{\theta^6 + 48\theta + 24x_i^4} - \sum_{i=1}^n x_i.$$

# Step 4: Set the derivative equal to zero and solve for the ML estimator

The value of  $\theta$  is obtained by solving the equation  $S(\theta; x_i) \stackrel{\text{set}}{=} 0$ , which involves setting the score function to zero:

$$S(\theta; x_i) = \frac{5n}{\theta} - \frac{10n\theta^4}{\theta^5 + 24} + \sum_{i=1}^n \frac{6\theta^5 + 48}{\theta^6 + 48\theta + 24x_i^4} - \sum_{i=1}^n x_i \stackrel{\text{set}}{=} 0.$$

This process identifies the critical points that may correspond to potential maxima of the log-likelihood function. Given the absence of a closed-form solution for the maximum likelihood (ML) estimator of the parameter, numerical iterative methods are employed to address the resulting non-linear optimization problem [21]. In this study, ML estimation was conducted using the Newton-Raphson method, as implemented through the maxLik package [15] in RStudio.

## 2.3. Confidence Intervals

This section presents four approaches for constructing confidence intervals (CIs) for the parameter of the XRani distribution: the likelihood-based CI, the Wald-type CI, the bootstrap-t CI, and the bias-corrected and accelerated (BCa) bootstrap CI.

## Likelihood-based Confidence Interval

The likelihood-based CI is a fundamental statistical technique used for parameter estimation. Central to this method is the likelihood function, which quantifies the probability of observing the data under a specified statistical model with given parameter values. The core idea is to identify a range of parameter values that maximize the likelihood while satisfying a predefined confidence level. This is achieved by maximizing the log-likelihood function with respect to the parameter of interest.

The ML estimator, denoted by  $\hat{\theta}$ , is obtained by solving the score equation:

$$S(\theta; x_i) \stackrel{\text{set}}{=} 0.$$

This estimator represents the parameter value most consistent with the observed data. Once the ML estimate is obtained, a likelihood-based CI is constructed around it. This method utilizes the likelihood ratio, defined as

$$\lambda(\theta) = \frac{L(\theta; x)}{L(\hat{\theta}; x)}.$$

Under regularity conditions, Wilks theorem states that  $-2 \log \lambda(\theta)$  asymptotically follows a chi-square distribution with degrees of freedom equal to the number of parameters estimated (typically 1 in this context) [26]. Thus, the likelihood-based CI for  $\theta$  at a



 $(1-\alpha)100\%$  confidence level is given by

$$\begin{split} & \left\{ \theta \left| -2 \log \frac{L(\theta; x)}{L(\hat{\theta}; x)} \leq \chi_{1-\alpha, 1}^{2} \right. \right\} \\ & = \left\{ \theta \left| -2 \log \left[ \frac{\theta^{5n} (\hat{\theta}^{5} + 24)^{2n}}{\hat{\theta}^{5n} (\theta^{5} + 24)^{2n}} \cdot \prod_{\substack{i=1 \\ n \ i=1}}^{n} (\hat{\theta}^{6} + 48\hat{\theta} + 24x_{i}^{4})} \exp \left( -\theta \sum_{i=1}^{n} x_{i} + \hat{\theta} \sum_{i=1}^{n} x_{i} \right) \right] \leq \chi_{1-\alpha, 1}^{2} \right\}, \end{split}$$

where  $\chi^2_{1-\alpha,1}$  is the critical value from the chi-square distribution with one degree of freedom.

For the XRani distribution, constructing the likelihood-based CI poses additional challenges due to the composite nature of the distribution. The inclusion of a gamma component with both shape and rate parameters increases the complexity of the likelihood function. To address this, numerical optimization methods are employed.

In this study, the ML estimator for the XRani distribution parameter was obtained using Brents root-finding algorithm. Given that:

$$f(\theta) = S(\theta; x_i) = \frac{5n}{\theta} - \frac{10n\theta^4}{\theta^5 + 24} + \sum_{i=1}^n \frac{6\theta^5 + 48}{\theta^6 + 48\theta + 24x_i^4} - \sum_{i=1}^n x_i^{\text{set}} 0.$$

Brents method was used to solve for  $\theta$  such that  $f(\theta) = 0$ . This algorithm integrates the robustness of bracketing methods—ensuring convergence—with the efficiency of open methods such as inverse quadratic interpolation. When the product  $f(a) \cdot f(b) < 0$ , the method begins with bisection to ensure reliability and then dynamically switches between interpolation techniques, depending on the curvature and interval behavior. Specifically, it alternates between inverse quadratic interpolation and the secant method (linear interpolation) to refine the root estimate iteratively:

$$\theta_{\text{second}} = \theta_n - f(\theta_n) \frac{\theta_n - \theta_{n-1}}{f(\theta_n) - f(\theta_{n-1})},$$

and secant technique (linear interpolation):

$$\theta_{\text{quad}} = \frac{f(\theta_{n-1})f(\theta_{n-2})}{(f(\theta_n) - f(\theta_{n-1}))(f(\theta_n) - f(\theta_{n-2}))}\theta_n + \dots$$

The likelihood-based CI employs an iterative process to improve the root estimate by alternating between multiple numerical methods. This approach enhances the stability and accuracy of the estimate [17].

Figure 3 illustrates the plot of the log-likelihood function versus  $\theta$  (solid blue line), the ML estimate (dashed red line), and the 95% likelihood-based CI (solid green line) for a simulated sample of size 20 from the XRani distribution with  $\theta = 1$ .

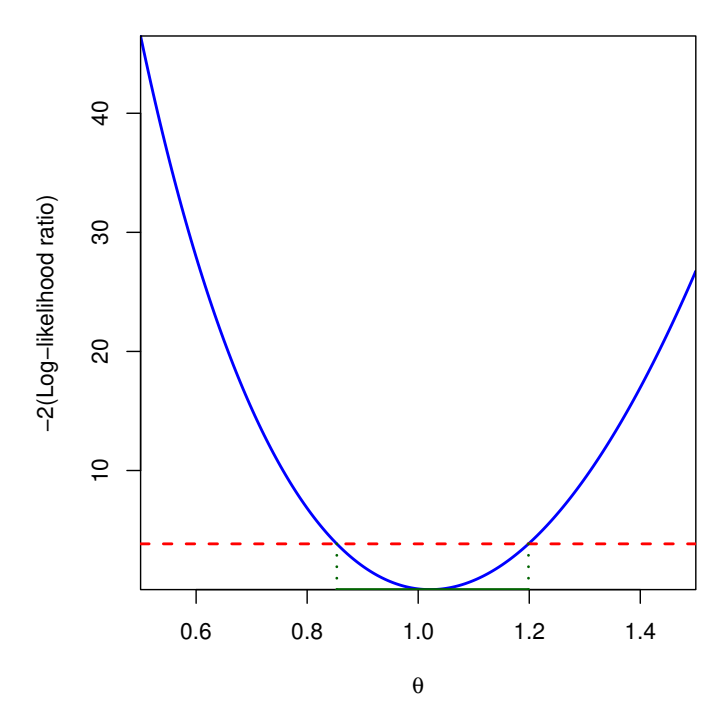


FIGURE 3. The plot of  $-2 \log \lambda(\theta)$  versus  $\theta$ .

## Wald-type Confidence Interval

The Wald-type CI for estimating the parameter of the XRani distribution is derived from the ML estimator, denoted by  $\hat{\theta}$ . This CI is constructed using a second-order Taylor series expansion of the log-likelihood function  $\log L(\theta;x)$  around  $\hat{\theta}$ . The approximation relies on the Wald statistic, which is based on the second derivative of the log-likelihood function, as the first derivative vanishes at the ML estimate:

$$\log L(\theta; x) \approx \log L(\hat{\theta}; x) - \frac{1}{2} I(\hat{\theta}) (\theta - \hat{\theta})^{2},$$

where  $I(\hat{\theta})$  is the observed Fisher information evaluated at  $\hat{\theta}$ . Under asymptotic conditions, where the sample size is sufficiently large, the Wald statistic provides an effective quadratic approximation to the likelihood ratio test (LRT) statistic [24]. For the XRani distribution, the first and second derivatives of the log-likelihood function are derived as follows:

$$\frac{\partial}{\partial \theta} \log L(\theta; x_i) = \frac{5n}{\theta} - \frac{10n\theta^4}{\theta^5 + 24} + \sum_{i=1}^n \frac{6\theta^5 + 48}{\theta^6 + 48\theta + 24x_i^4} - \sum_{i=1}^n x_i,$$



$$\frac{\partial^2}{\partial \theta^2} \log L(\theta; x_i) = -\frac{5n}{\theta^2} - \frac{40n\theta^3}{\theta^5 + 24} + \frac{50n\theta^8}{(\theta^5 + 24)^2} + \sum_{i=1}^n \frac{30\theta^4}{\theta^6 + 48\theta + 24x_i^4} - \sum_{i=1}^n \frac{(6\theta^5 + 48)^2}{(\theta^6 + 48\theta + 24x_i^4)^2}.$$

Consequently, the observed Fisher information is estimated as:

$$\hat{I}(\hat{\theta}) = -\frac{\partial^2}{\partial \theta^2} \log L(\theta; x_i) \bigg|_{\theta = \hat{\theta}}.$$
(2.2)

The Wald-type confidence interval for  $\theta$  at a confidence level of  $(1-\alpha)100\%$  is given by

$$\left(\hat{\theta}-z_{1-(\alpha/2)}\sqrt{\hat{I}^{-1}(\hat{\theta})},\hat{\theta}+z_{1-(\alpha/2)}\sqrt{\hat{I}^{-1}(\hat{\theta})}\right),$$

where  $z_{1-(\alpha/2)}$  denotes the  $(1-(\alpha/2))^{\text{th}}$  quantile of the standard normal distribution, and  $\hat{I}^{-1}(\hat{\theta})$  is the inverse of the observed Fisher information given in Equation 2.2.

## Bootstrap-t Confidence Interval

The bootstrap-t CI is a resampling-based method that estimates the uncertainty around a parameter by combining the bootstrap technique with the t-distribution framework. Unlike the traditional percentile bootstrap, the bootstrap-t method incorporates the variability of the estimator through its standard error, thereby improving accuracy and robustness—particularly in small sample settings or when the sampling distribution of the estimator departs from normality [8].

This method is especially useful when the analytical form of the sampling distribution is complex or unknown. The CI is constructed based on the empirical distribution of a standardized statistic, also known as the bootstrap-t statistic, which approximates the pivotal quantity used in parametric inference.

The steps for constructing a bootstrap-t CI are as follows:

#### Step 1: Initial Estimation

Begin by drawing a random sample  $X = (X_1, ..., X_n)$  from the population. Compute the point estimate  $\hat{\theta}$  of the parameter of interest (e.g., ML estimate).

#### Step 2: Bootstrap Sampling

Generate B=1000 bootstrap samples,  $X_b^*$ , b=1,2,...,B, by sampling with replacement from the original dataset.

#### Step 3: Parameter Estimation for Each Sample

For each bootstrap sample  $X_b^*$ , compute the bootstrap replicate of the estimator, denoted as  $\hat{\theta}_b^*$ .

## Step 4: Construct the Bootstrap-t Statistic

For each bootstrap replicate, calculate the standardized statistic (bootstrap-t) as:

$$t_b^* = \frac{\hat{\theta}_b^* - \hat{\theta}}{\widehat{SE}_b^*},$$

where  $\widehat{\mathrm{SE}}_b^* = \sqrt{\widehat{I}^{-1}(\widehat{\theta}_b^*)}$  is the bootstrap estimate of the standard error of  $\widehat{\theta}_b^*$ , often obtained via the observed Fisher information (see Equation 2.2), with the parameter substituted by  $\widehat{\theta}_b^*$ .

## Step 5: Construct the Empirical Distribution

Repeat steps 2-4 a total of B = 1000 times to obtain the empirical distribution of the  $t_b^*$  values. This distribution approximates the sampling distribution of the standardized estimator.

## Step 6: Quantile Calculation

Determine the lower and upper quantiles  $t_{\alpha/2}^*$  and  $t_{1-\alpha/2}^*$  corresponding to the  $\alpha/2$  and  $1-(\alpha/2)$  levels of the empirical bootstrap-t distribution. That is,

$$t_{\alpha/2}^* = \inf \left\{ t : \frac{1}{B} \sum_{b=1}^B \mathbf{1}_{[t_b^* \le t]} \ge \alpha/2 \right\}$$

and

$$t_{1-(\alpha/2)}^* = \inf \left\{ t : \frac{1}{B} \sum_{b=1}^B \mathbf{1}_{[t_b^* \le t]} \ge 1 - (\alpha/2) \right\},$$

where  $\mathbf{1}_{[.]}$  is the indicator function.

## Step 7: Construct the Bootstrap-t Confidence Interval

The two-sided  $(1-\alpha)100\%$  bootstrap-t confidence interval is given by

$$\left(\widehat{\theta} - t_{1-(\alpha/2)}^* \cdot \widehat{\mathrm{SE}}(\widehat{\theta}), \ \widehat{\theta} - t_{\alpha/2}^* \widehat{\mathrm{SE}}(\widehat{\theta})\right),$$

where  $\widehat{\text{SE}}(\hat{\theta}) = \sqrt{\hat{I}^{-1}(\hat{\theta})}$  is the standard error of the original estimator  $\hat{\theta}$ .

## Bias-corrected and accelerated (BCa) bootstrap confidence interval

The bias-corrected and accelerated (BCa) bootstrap CI is a refined extension of the basic bootstrap approach that corrects for both bias and skewness in the empirical distribution of the estimator. This method is particularly advantageous in situations involving small sample sizes or when the distribution of the estimator is notably non-normal. It improves interval estimation accuracy by incorporating two essential adjustments: (1) a bias correction factor to account for the asymmetry in the proportion of bootstrap replicates falling below the original estimate, and (2) an acceleration parameter that adjusts for the curvature (skewness) in the estimators distribution [3]. Unlike standard methods that assume normality or symmetry in the sampling distribution, the BCa method does not require such assumptions, making it highly robust and broadly applicable.

The construction of the BCa bootstrap CI proceeds as follows:

#### Step 1: Initial Estimation

Draw a random sample  $X = (X_1, ..., X_n)$  from the population. Estimate the parameter of interest  $\hat{\theta}$  using a suitable method, such as maximum likelihood.

## Step 2: Bootstrap Resampling

Generate B=1000 bootstrap samples  $X_b^*$ , b=1,2,...,B, by sampling with replacement from the original dataset.

#### Step 3: Bootstrap Estimation



For each bootstrap sample, compute the bootstrap estimator  $\hat{\theta}_b^*$ , yielding a distribution of bootstrap estimates  $\left\{\hat{\theta}_1^*, \hat{\theta}_2^*, ..., \hat{\theta}_B^*\right\}$ .

## Step 4: Bias Correction Factor $(z_0)$

Calculate the proportion  $\hat{p}$  of bootstrap estimates that are less than the original estimate  $\hat{\theta}$ :

$$\hat{p} = \frac{1}{B} \sum_{b=1}^{B} \mathbf{1}_{[\hat{\theta}_b^* < \hat{\theta}]}.$$

The bias correction factor  $z_0$  is then obtained as the standard normal quantile:

$$z_0 = \Phi^{-1}(\hat{p}),$$

where  $\Phi^{-1}(\cdot)$  is the inverse of the standard normal cumulative distribution function.

## Step 5: Acceleration Constant (a)

Estimate the acceleration constant a, which reflects the rate of change of the standard error of the estimator with respect to the data. It is typically obtained using the jackknife method:

$$a = \frac{\sum_{i=1}^{n} (\bar{\theta}_{(\cdot)} - \hat{\theta}_{(i)})^{3}}{6 \left[\sum_{i=1}^{n} (\bar{\theta}_{(\cdot)} - \hat{\theta}_{(i)})^{2}\right]^{3/2}},$$

where  $\hat{\theta}_{(i)}$  is the leave-one-out estimate, and  $\bar{\theta}_{(\cdot)}$  is their average.

## Step 6: Adjusted Percentiles

The corrected quantiles  $\alpha_1$  and  $\alpha_2$  for the confidence interval are calculated as:

$$\alpha_1 = \Phi\left(z_0 + \frac{z_0 + z_{\alpha/2}}{1 - a(z_0 + z_{\alpha/2})}\right)$$
 and  $\alpha_2 = \Phi\left(z_0 + \frac{z_0 + z_{1-(\alpha/2)}}{1 - a(z_0 + z_{1-(\alpha/2)})}\right)$ ,

where  $z_{\alpha/2}$  and  $z_{1-\alpha/2}$  are the  $(\alpha/2)^{\text{th}}$  and  $(1-(\alpha/2))^{\text{th}}$  quantiles of the standard normal distribution, respectively.

#### Step 7: BCa Bootstrap Confidence Interval Construction

Finally, the two-sided  $(1-\alpha)100\%$  BCa bootstrap CI is constructed using the adjusted percentiles  $\alpha_1$  and  $\alpha_2$  as:

$$\left(\hat{\theta}_{(\alpha_1)}^*, \hat{\theta}_{(\alpha_2)}^*\right),$$

where  $\hat{\theta}_{(\alpha_1)}^*$  and  $\hat{\theta}_{(\alpha_2)}^*$  are  $(\alpha_1)^{\text{th}}$  and  $(\alpha_2)^{\text{th}}$  quantiles of the sorted bootstrap estimates  $\hat{\theta}_b^*$ .

This study did not investigate Bayesian credible intervals for the XRani distribution due to both methodological and practical considerations. First, the XRani distribution is relatively new and does not yet have well-established conjugate or informative priors in the literature. The choice of a prior distribution is a critical step in Bayesian analysis, as it can substantially influence posterior inference [12]. Developing and justifying such priors for the XRani distribution would require a separate methodological study. Second, the likelihood function of the XRani distribution involves a mixture structure with polynomial and exponential terms, making the posterior analytically intractable.

As a result, Bayesian credible intervals would require computationally intensive simulation techniques such as Markov Chain Monte Carlo (MCMC) [25], along with careful convergence diagnostics [4], which are beyond the scope of the present research. Since the primary objective of this work is to compare frequentist CI procedures—likelihood-based, Wald-type, bootstrap—t, and BCa bootstrap—under both simulated and real-world data situations, we focused exclusively on methods consistent with this framework. Future work may explore Bayesian inference for the XRani distribution, especially in contexts where informative priors can be elicited from domain expertise or historical data.

In the case of the XRani distribution, which involves a single parameter  $\theta$ , the profile likelihood CI is mathematically equivalent to the likelihood-based CI because the profiling process over nuisance parameters is unnecessary. As a result, both approaches yield identical interval estimates [24].

## 3. Simulation Studies and Results

This study proposes 95% two-sided confidence intervals (CIs) for the parameter of the XRani distribution, constructed using four distinct methods: likelihood-based, Wald-type, bootstrap-t, and bias-corrected and accelerated (BCa) bootstrap. The efficiency and reliability of these methods were systematically evaluated through a Monte Carlo simulation study implemented in RStudio, under a range of controlled scenarios.

The performance of the proposed CIs was assessed using two key metrics: empirical coverage probability (ECP) and average width (AW), with the number of bootstrap replicates fixed at B=2,000. The considered sample sizes were  $n=10,\,20,\,30,\,50,\,100,\,200,\,300,\,$  and 500. Although n=10 represents a challenging estimation scenario, its inclusion enables an evaluation of method robustness under extreme small-sample conditions. The initial analysis focused on n=200, representative of typical moderate-scale field studies. To examine asymptotic behavior, an additional simulation with n=500 was conducted, which confirmed the stability and convergence trends observed in earlier settings.

The true parameter values  $\theta$  of the XRani distribution were set to 0.20, 0.30, 0.50, 0.75, 1.00, 1.50, 2.00, and 2.50. For each combination of sample size and parameter value, the simulation was repeated 2,000 times to ensure robustness and statistical validity.

The simulation results, as summarized in Table 1 and 2 and visualized in Figures 4 and 5, provide a detailed comparative evaluation of the ECPs and AWs of four competing 95% two-sided CI estimation methods for the parameter of the XRani distribution: likelihood-based, Wald-type, bootstrap-t, and BCa bootstrap. Across all parameter values and sample sizes, the likelihood-based and Wald-type CIs demonstrated superior performance in terms of coverage accuracy, with ECPs consistently aligning with or slightly exceeding the nominal confidence level of 0.95. These two methods remained particularly robust as the sample size increased, showing a convergence of ECPs toward the nominal level even at moderate sample sizes such as n=30.

In contrast, the bootstrap-t and BCa bootstrap methods exhibited notably lower ECPs at smaller sample sizes (n=10,20,30) frequently underestimating the nominal confidence level. This undercoverage highlights the sensitivity of these resampling-based methods to limited data, especially in the presence of distributional skewness or kurtosis. However, as the sample size increased to n=100 and n=200, the performance of both bootstrap methods improved substantially, with their ECPs gradually converging to levels comparable with those of the likelihood-based and Wald-type CIs. This suggests that

bootstrap-based CIs are asymptotically valid but may be unreliable for small samples unless corrections or alternatives are applied.

With respect to AW, the simulation results revealed a clear trend: as the true parameter value increased, so did the width of the CIs, which is expected due to increased uncertainty in estimation at higher parameter levels. Among the four methods, the bootstrap-t and BCa bootstrap CIs consistently yielded narrower intervals compared to the likelihood-based and Wald-type approaches. This reflects a potential trade-off between precision and reliability—while narrower intervals imply greater efficiency, they were also associated with lower ECPs, particularly at small sample sizes.

Overall, the simulation results underscore several key insights: The likelihood-based and Wald-type methods are preferable for maintaining nominal coverage, especially in small to moderate samples. The bootstrap-t and BCa methods may offer narrower intervals, but at the cost of reduced coverage reliability unless sufficiently large sample sizes are used. For high parameter values or skewed distributions, likelihood-based inference remains the most robust, with the BCa bootstrap method showing improved performance in larger samples due to its bias and skewness adjustments. These findings support the use of hybrid approaches that leverage the flexibility of bootstrap resampling while incorporating asymptotic corrections to enhance coverage properties.

TABLE 1. Empirical coverage probability and average width of the 95% two-sided CIs for the parameter of the XRani distribution ( $\theta = 0.20$ , 0.30, 0.50, and 0.75)

$\theta$	n	Empirica	l Covera	ge Proba	bility	I	Average V	Width	
		Likelihood	Wald	Boot-t	BCa	Likelihood	Wald	Boot-t	BCa
0.20	10	0.9585	0.9630	0.9095	0.9110	0.1143	0.1140	0.1021	0.1050
	20	0.9445	0.9475	0.9255	0.9190	0.0804	0.0803	0.0755	0.0763
	30	0.9525	0.9565	0.9265	0.9350	0.0654	0.0654	0.0612	0.0619
	50	0.9620	0.9645	0.9495	0.9480	0.0502	0.0502	0.0476	0.0479
	100	0.9530	0.9565	0.9355	0.9340	0.0356	0.0356	0.0333	0.0334
	200	0.9440	0.9420	0.9365	0.9375	0.0249	0.0249	0.0243	0.0243
	300	0.9450	0.9475	0.9370	0.9340	0.0204	0.0204	0.0198	0.0198
	500	0.9570	0.9570	0.9535	0.9560	0.0157	0.0157	0.0154	0.0154
0.30	10	0.9575	0.9625	0.9015	0.9025	0.1719	0.1716	0.1530	0.1579
	20	0.9550	0.9615	0.9250	0.9265	0.1208	0.1207	0.1136	0.1152
	30	0.9635	0.9690	0.9380	0.9455	0.0971	0.0970	0.0912	0.0918
	50	0.9620	0.9635	0.9345	0.9315	0.0755	0.0754	0.0683	0.0686
	100	0.9625	0.9620	0.9465	0.9450	0.0531	0.0531	0.0496	0.0498
	200	0.9560	0.9600	0.9470	0.9460	0.0376	0.0376	0.0362	0.0363
	300	0.9625	0.9665	0.9490	0.9500	0.0305	0.0305	0.0289	0.0290
	500	0.9590	0.9610	0.9560	0.9540	0.0235	0.0235	0.0234	0.0235

$\theta$	n	Empirica	l Covera	ge Proba	bility	I	Average V	Width	
		Likelihood	Wald	Boot-t	BCa	Likelihood	Wald	Boot-t	BCa
0.50	10	0.9550	0.9590	0.8960	0.9105	0.2808	0.2806	0.2494	0.2553
	20	0.9530	0.9590	0.9145	0.9220	0.1966	0.1965	0.1863	0.1880
	30	0.9665	0.9675	0.9360	0.9365	0.1603	0.1603	0.1472	0.1479
	50	0.9435	0.9500	0.9285	0.9205	0.1270	0.1270	0.1191	0.1194
	100	0.9535	0.9525	0.9400	0.9420	0.0878	0.0878	0.0826	0.0829
	200	0.9575	0.9610	0.9480	0.9475	0.0623	0.0622	0.0590	0.0590
	300	0.9425	0.9480	0.9345	0.9340	0.0509	0.0509	0.0492	0.0493
	500	0.9575	0.9565	0.9520	0.9530	0.0391	0.0391	0.0386	0.0387
0.75	10	0.9470	0.9460	0.8885	0.8865	0.4027	0.4046	0.3646	0.3636
	20	0.9510	0.9480	0.9125	0.9155	0.2839	0.2845	0.2611	0.2601
	30	0.9425	0.9480	0.9200	0.9125	0.2354	0.2357	0.2241	0.2233
	50	0.9590	0.9580	0.9350	0.9405	0.1799	0.1801	0.1725	0.1723
	100	0.9470	0.9485	0.9340	0.9310	0.1272	0.1272	0.1226	0.1227
	200	0.9555	0.9580	0.9440	0.9410	0.0900	0.0901	0.0858	0.0858
	300	0.9505	0.9540	0.9445	0.9440	0.0733	0.0733	0.0723	0.0724
	500	0.9620	0.9600	0.9540	0.9520	0.0565	0.0565	0.0555	0.0557

Table 2. Empirical coverage probability and average width of the 95% two-sided CIs for the parameter of the XRani distribution ( $\theta=1.00,$  1.50, 2.00, and 2.50)

$\theta$	n	Empirica	l Covera	ge Proba	bility	I	Average V	Width	
		Likelihood	Wald	Boot-t	BCa	Likelihood	Wald	Boot-t	BCa
1.00	10	0.9620	0.9570	0.9025	0.8920	0.4807	0.4839	0.4382	0.4347
	20	0.9580	0.9560	0.9265	0.9185	0.3433	0.3445	0.3210	0.3186
	30	0.9475	0.9475	0.9300	0.9260	0.2807	0.2815	0.2673	0.2654
	50	0.9455	0.9460	0.9305	0.9275	0.2164	0.2168	0.2089	0.2079
	100	0.9520	0.9530	0.9430	0.9395	0.1539	0.1540	0.1480	0.1477
	200	0.9405	0.9410	0.9385	0.9355	0.1088	0.1088	0.1086	0.1086
	300	0.9515	0.9505	0.9395	0.9390	0.0887	0.0887	0.0886	0.0886
	500	0.9615	0.9615	0.9500	0.9475	0.0687	0.0687	0.0650	0.0651
1.50	10	0.9490	0.9585	0.8970	0.9365	0.5800	0.5739	0.5238	0.5841
	20	0.9540	0.9560	0.9315	0.9415	0.4022	0.4004	0.3768	0.3916
	30	0.9530	0.9550	0.9380	0.9495	0.3271	0.3262	0.3148	0.3235
	50	0.9575	0.9600	0.9400	0.9465	0.2528	0.2524	0.2450	0.2488
	100	0.9530	0.9550	0.9550	0.9535	0.1779	0.1778	0.1769	0.1785
	200	0.9440	0.9455	0.9400	0.9390	0.1259	0.1259	0.1227	0.1235
	300	0.9590	0.9585	0.9445	0.9520	0.1022	0.1021	0.0987	0.0991
	500	0.9515	0.9500	0.9415	0.9435	0.0791	0.0791	0.0775	0.0777

$\theta$	n	Empirica	l Covera	ge Proba	bility	I	Average V	Width	
		Likelihood	Wald	Boot-t	BCa	Likelihood	Wald	Boot-t	BCa
2.00	10	0.9460	0.9690	0.8985	0.8825	1.1259	1.0570	0.8711	1.2383
	20	0.9530	0.9725	0.9245	0.9385	0.6781	0.6559	0.5859	0.6949
	30	0.9525	0.9670	0.9280	0.9450	0.5288	0.5178	0.4765	0.5305
	50	0.9560	0.9630	0.9345	0.9530	0.3989	0.3942	0.3746	0.3985
	100	0.9500	0.9545	0.9430	0.9490	0.2753	0.2738	0.2662	0.2741
	200	0.9630	0.9665	0.9610	0.9615	0.1913	0.1908	0.1865	0.1892
	300	0.9510	0.9530	0.9425	0.9455	0.1551	0.1549	0.1513	0.1530
	500	0.9480	0.9485	0.9490	0.9525	0.1192	0.1191	0.1184	0.1193
2.50	10	0.9510	0.9585	0.9095	0.8135	2.4297	2.3545	1.9336	2.3810
	20	0.9500	0.9570	0.9325	0.8640	1.5059	1.4588	1.2970	1.4342
	30	0.9560	0.9645	0.9405	0.8960	1.1636	1.1303	1.0328	1.1134
	50	0.9505	0.9615	0.9450	0.9180	0.8537	0.8347	0.7801	0.8258
	100	0.9515	0.9620	0.9430	0.9355	0.5663	0.5583	0.5333	0.5546
	200	0.9460	0.9465	0.9365	0.9390	0.3871	0.3842	0.3740	0.3828
	300	0.9525	0.9540	0.9475	0.9485	0.3132	0.3115	0.3045	0.3096
	500	0.9490	0.9495	0.9455	0.9470	0.2409	0.2401	0.2367	0.2398

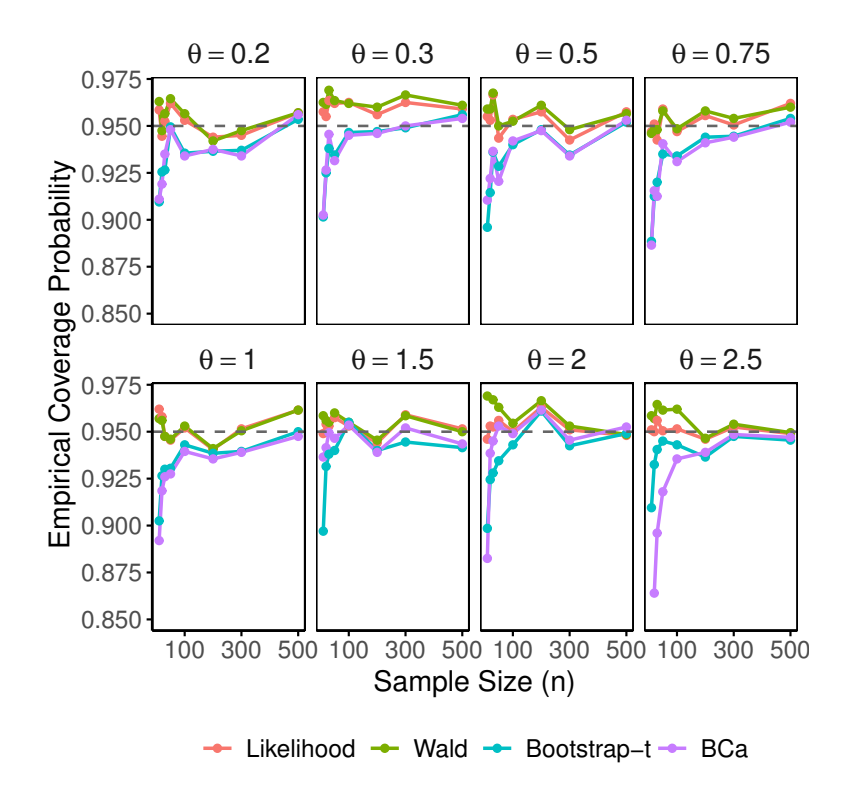


FIGURE 4. Plots of the ECPs of the CIs for the parameter of the XRani distribution.

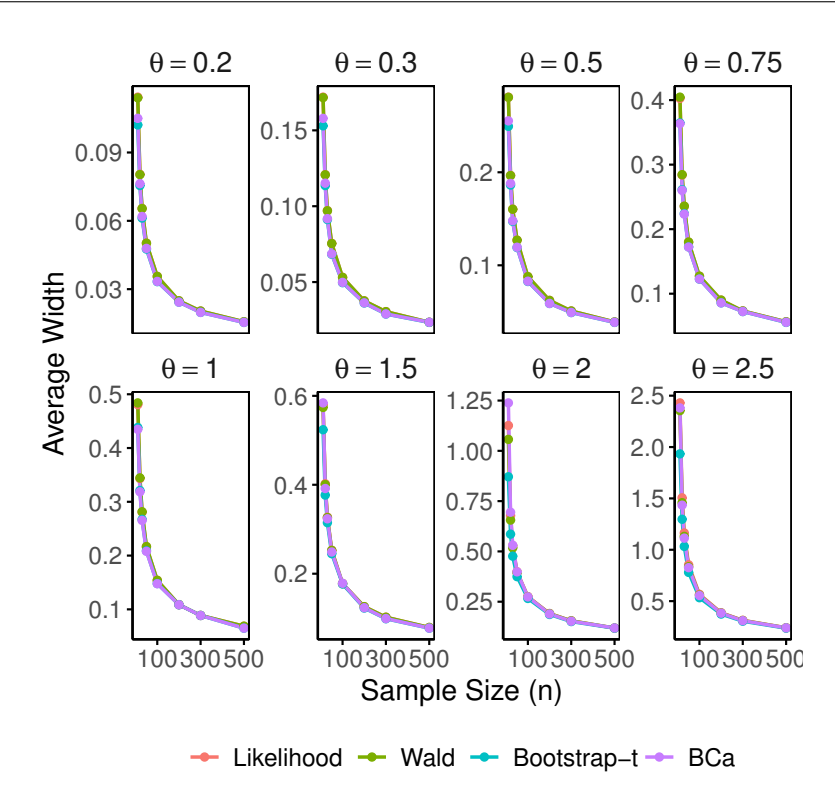


FIGURE 5. Plots of the AWs of the CIs for the parameter of the XRani distribution

## 4. Real Data Applications

To demonstrate the practical applicability of the CI estimation methods for the parameter of the XRani distribution, we applied them to two real data sets. The suitability of the XRani distribution was further evaluated by comparing its performance with fourteen alternative distributions. All these PDFs are defined for x > 0 and are characterized by a single parameter  $\theta > 0$ :

(1) The Akash distribution [29]

$$f(x;\theta) = \frac{\theta^3}{\theta^2 + 2} (1 + x^2) e^{-\theta x}.$$

(2) The Akshaya distribution [35]

$$f(x;\theta) = \frac{\theta^4}{\theta^3 + 3\theta^2 + 6\theta + 6} (1+x)^3 e^{-\theta x}.$$

(3) The Amarendra distribution [31]

$$f(x;\theta) = \frac{\theta^4}{\theta^3 + \theta^2 + 2\theta + 6} (1 + x + x^2 + x^3) e^{-\theta x}.$$



(4) The Sujatha distribution [32]

$$f(x;\theta) = \frac{\theta^3}{\theta^2 + \theta + 2} \left( 1 + x + x^2 \right) e^{-\theta x}.$$

(5) The Shanker distribution [28]

$$f(x;\theta) = \frac{\theta^2}{\theta^2 + 1}(\theta + x)e^{-\theta x}.$$

(6) The Adya distribution [40]

$$f(x;\theta) = \frac{\theta^3}{\theta^4 + 2\theta^2 + 2} (\theta + x)^2 e^{-\theta x}.$$

(7) The Garima distribution [33]

$$f(x;\theta) = \frac{\theta}{\theta + 2} (1 + \theta + \theta x) e^{-\theta x}.$$

(8) The Komal distribution [38]

$$f(x;\theta) = \frac{\theta^2}{\theta^2 + \theta + 1} (1 + \theta + x) e^{-\theta x}.$$

(9) The Ishita distribution [36]

$$f(x;\theta) = \frac{\theta^3}{\theta^3 + 2} (\theta + x^2) e^{-\theta x}.$$

(10) The Iwok-Nwikpe distribution [16]

$$f(x;\theta) = \frac{\theta^3}{\theta + 2}(x^2 + x)e^{-\theta x}.$$

(11) The Pratibha distribution [39]

$$f(x;\theta) = \frac{\theta^3}{\theta^3 + \theta + 2} (\theta + x + x^2) e^{-\theta x}.$$

(12) The Chris-Jerry distribution [23]

$$f(x;\theta) = \frac{\theta^2}{\theta + 2} (1 + \theta x^2) e^{-\theta x}.$$

(13) The Lindley distribution [14]

$$f(x;\theta) = \frac{\theta^2}{\theta + 1}(1+x)e^{-\theta x}.$$

(14) The exponential distribution

$$f(x;\theta) = \theta e^{-\theta x}$$
.

## 4.1. Daily Average PM2.5 Concentrations in Bang Kapi District

The data consist of daily average PM2.5 concentrations (in  $\mu g/m^3$ ) recorded in Bang Kapi District, Bangkok, from January to April 2024, provided by the Thai Meteorological Department. The dataset comprises 91 observations as follows:

 $28.2, 25.8, 26.3, 31.1, 30.1, 33.9, 34.8, 39.6, 57.4, 48.7, 36.0, 26.1, 28.3, 34.5, 27.3, 33.6, \\ 36.2, 41.5, 48.5, 50.3, 35.8, 38.2, 50.4, 24.7, 24.1, 32.7, 45.0, 50.3, 37.1, 61.1, 64.0, 37.0, \\ 23.8, 24.0, 26.0, 31.5, 24.9, 25.1, 21.9, 20.8, 36.3, 35.2, 55.5, 71.0, 76.6, 57.1, 30.2, 23.3, \\ 17.7, 14.7, 12.7, 13.1, 13.6, 13.7, 16.0, 17.1, 27.6, 36.4, 22.0, 17.9, 21.1, 25.1, 24.3, 23.2, \\ 20.9, 19.6, 24.0, 20.9, 19.9, 17.4, 32.8, 26.2, 20.7, 19.7, 18.4, 18.7, 18.4, 25.5, 26.5, 34.4, \\ 50.2, 40.3, 17.1, 19.6, 20.0, 17.0, 18.2, 17.1, 21.0, 13.2, 13.3.$ 

Descriptive statistics for this dataset are summarized in Table 3, while Figure 6 provides visual representations, including a histogram, Box and Whisker plot, kernel density plot, and violin plot, effectively highlighting the datasets positive skewness.

Table 3. Descriptive statistics for the PM2.5 concentrations in Bang Kapi District

Sample Sizes	Minimum	Q1	Median	Mean	Q3	Maximum	St.Dev
91	12.70	19.95	26.00	29.99	36.10	76.60	13.7117

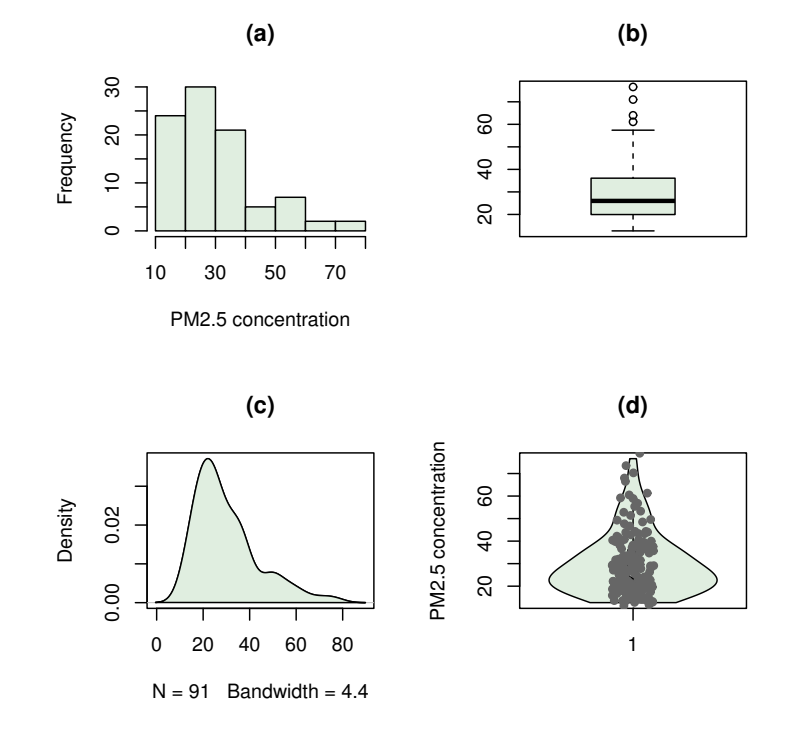


FIGURE 6. Visual representations of the PM2.5 concentration data in Bang Kapi District: (a) Histogram, (b) Box and Whisker plot, (c) Kernel density plot, and (d) Violin plot.

The parameter of the XRani distribution was estimated using the ML estimation method. Subsequently, four types of 95% CIs for the distribution parameter were constructed, namely: likelihood-based CI, Wald-type CI, bootstrap-t CI, and BCa bootstrap CI

A comprehensive evaluation was performed using multiple criteria, including the log-likelihood ( $\log(\hat{L})$ ), the Akaike information criterion (AIC), and the Bayesian information criterion (BIC), referred to as the Schwarz information criterion. These criteria allowed for an objective assessment of model adequacy across the different distributions. The AIC and BIC are defined as:

$$AIC = 2k - 2\log \hat{L}$$
 and  $BIC = 2k\log(n) - 2\log \hat{L}$ ,

where k represents the number of estimated parameters in the model and  $\hat{L}$  denotes the maximized value of the likelihood function for the model. A distribution with lower AIC and BIC values is generally preferred, as these statistics indicate a better balance between model fit and complexity. Table 4 provides the parameter estimates, along with their corresponding standard errors (SEs) and goodness-of-fit measures, for the dataset under investigation.

Table 4. Comparative analysis of model fit statistics for different distributions applied to PM2.5 concentration data in Bang Kapi district

Distribution	Estimate (SE)	LogLik	AIC	BIC
XRani	0.1667 (0.0078)	-354.684	711.367	713.878
Akash	0.0997 (0.0060)	-362.567	727.133	729.644
Akshaya	$0.1291 \ (0.0068)$	-358.222	718.444	720.955
Amarendra	$0.1318 \; (0.0069)$	-357.411	716.821	719.332
Aradhana	$0.0968 \ (0.0059)$	-364.152	730.304	732.815
Sujatha	$0.0982 \ (0.0059)$	-363.413	728.825	731.336
Adya	$0.0996 \ (0.0060)$	-362.467	726.934	729.445
Garima	$0.0523 \ (0.0047)$	-391.971	785.942	788.452
Komal	$0.0645 \ (0.0048)$	-376.033	754.066	756.577
Ishita	$0.1000 \ (0.0060)$	-362.309	726.618	729.129
Iwok-Nwikpe	$0.0985 \ (0.0060)$	-363.152	728.305	730.816
Pratibha	$0.0984 \ (0.0060)$	-363.178	728.356	730.867
Chris-Jerry	0.0979(0.0060)	-365.017	732.033	734.544
Lindley	$0.0665 \ (0.0049)$	-375.971	753.942	756.452
Exponential	0.0333 (0.0035)	-400.476	802.951	805.462

Note. Bold values indicate the best-fitting model based on minimum AIC and BIC values.

Table 4 presents the log-likelihood values along with the AIC and BIC for the XRani distribution and fourteen alternative distributions fitted to the PM2.5 concentration data. Among the compared distributions, the XRani distribution exhibited the best overall fit, as indicated by the lowest AIC and BIC values.

A goodness-of-fit test was conducted using the KolmogorovSmirnov (KS) statistic [7] to assess whether the PM2.5 concentration data in Bang Kapi District follow the XRani distribution. The test yielded a KS statistic of 0.0971 and a p-value of 0.3572. Since the

p-value exceeds the 0.05 significance level, there is insufficient evidence to reject the null hypothesis, indicating that the XRani distribution provides an adequate fit to the data.

Furthermore, the ProbabilityProbability (PP) plot in Figure 7 compares the empirical cumulative distribution function (CDF) of the observed data with the theoretical CDF of the XRani distribution based on the estimated parameter. The plotted points lie closely along the 45-degree reference line, indicating good agreement between the empirical and theoretical distributions. This visual evidence supports the adequacy of the XRani distribution in modeling the given dataset.

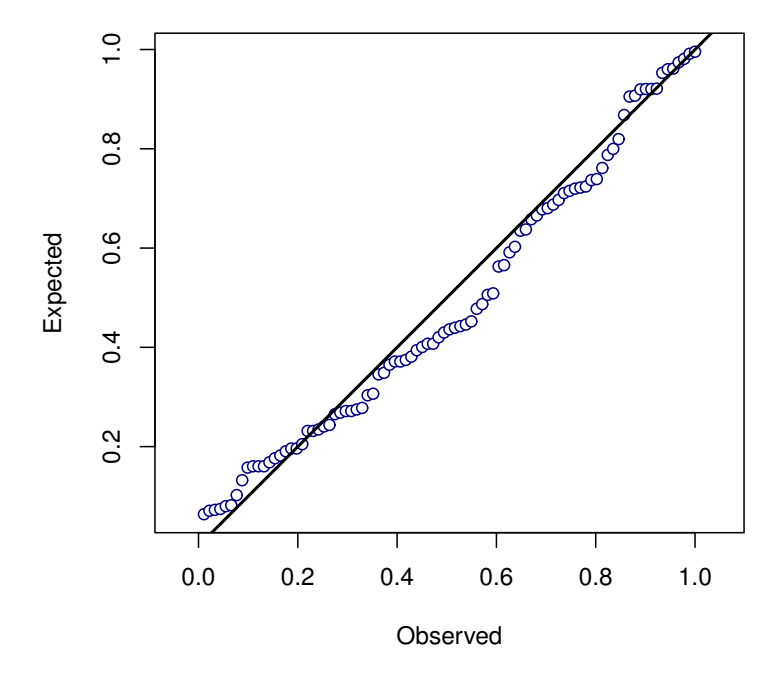


FIGURE 7. P-P plot of the PM2.5 concentration data in Bang Kapi District.

The ML estimate of the XRani distribution parameter was 0.1667. To further assess the uncertainty associated with the parameter estimate, Table 5 reports the 95% two-sided CIs for the XRani distribution parameter, constructed using four different methods. The likelihood-based method produced a 95% CI of (0.1519, 0.1825), with an interval width of 0.0306. The Wald-type method yielded a similar interval, ranging from 0.1514 to 0.1820, with the same width of 0.0306. In contrast, the bootstrap-t and BCa bootstrap methods resulted in slightly wider intervals—(0.1514, 0.1832) and (0.1506, 0.1819), respectively.

These findings demonstrate not only the suitability of the XRani distribution for modeling PM2.5 concentrations but also the advantages of using likelihood-based and Wald-type methods for interval estimation, particularly in moderate sample settings.

95% CI 99% CI CI Method Interval Width Interval Width Likelihood-based (0.1519, 0.1825)0.0306(0.1474, 0.1877)0.0403Wald-type (0.1514, 0.1820)0.0306(0.1466, 0.1869)0.0403(0.1483, 0.1865)0.0382 Bootstrap-t (0.1514, 0.1832)0.0318(0.1506, 0.1819)BCa bootstrap (0.1468, 0.1878)0.04100.0313

TABLE 5. The 95% and 99% two-sided CIs and corresponding widths for the XRani parameter based on PM2.5 data in Bang Kapi District

#### 4.2. Daily Average PM2.5 Concentrations in Phaya Thai District

Ninety-one daily mean PM2.5 measurements ( $\mu g/m^3$ ) taken in Phaya Thai District, Bangkok, during JanuaryApril 2024 were obtained from the Thai Meteorological Department. The following are the recorded data:

 $22.0,\ 21.4,\ 21.4,\ 22.9,\ 20.6,\ 25.9,\ 25.1,\ 28.9,\ 39.9,\ 29.6,\ 24.1,\ 20.4,\ 21.2,\ 27.2,\ 22.0,\ 22.8,\ 28.8,\ 33.1,\ 40.5,\ 33.0,\ 27.4,\ 30.1,\ 38.0,\ 19.1,\ 20.4,\ 24.8,\ 33.2,\ 36.6,\ 30.8,\ 49.3,\ 44.3,\ 24.4,\ 19.4,\ 19.4,\ 21.3,\ 26.5,\ 22.7,\ 19.3,\ 18.6,\ 17.1,\ 28.5,\ 28.6,\ 45.2,\ 50.3,\ 53.3,\ 42.7,\ 24.2,\ 19.0,\ 15.1,\ 14.0,\ 10.9,\ 12.8,\ 12.6,\ 12.3,\ 15.0,\ 14.9,\ 21.9,\ 28.3,\ 17.4,\ 16.4,\ 16.8,\ 20.3,\ 20.4,\ 20.1,\ 19.2,\ 16.2,\ 21.6,\ 18.0,\ 18.8,\ 14.0,\ 29.3,\ 23.5,\ 18.9,\ 17.8,\ 16.3,\ 16.1,\ 16.3,\ 20.2,\ 24.3,\ 27.8,\ 33.5,\ 39.2,\ 15.7,\ 18.9,\ 20.2,\ 16.7,\ 15.5,\ 14.8,\ 21.6,\ 13.6,\ 12.6.$ 

Summary measures of the dataset are presented in Table 6, and the distributional characteristics are illustrated in Figure 8, which reveals a noticeable right-skewed pattern in the data.

Table 6. Descriptive statistics for the PM2.5 concentrations in Phaya Thai District

Sample Sizes	Minimum	Q1	Median	Mean	Q3	Maximum	St.Dev
91	10.90	17.60	21.40	23.90	28.40	53.30	9.1891

Model adequacy was thoroughly examined using various indicators, such as the log-likelihood  $(\log(\hat{L}))$ , along with information-based metrics including AIC and BIC. As shown in Table 7, the estimated parameters, their standard errors (SEs), and relevant model evaluation metrics are presented for the given dataset.

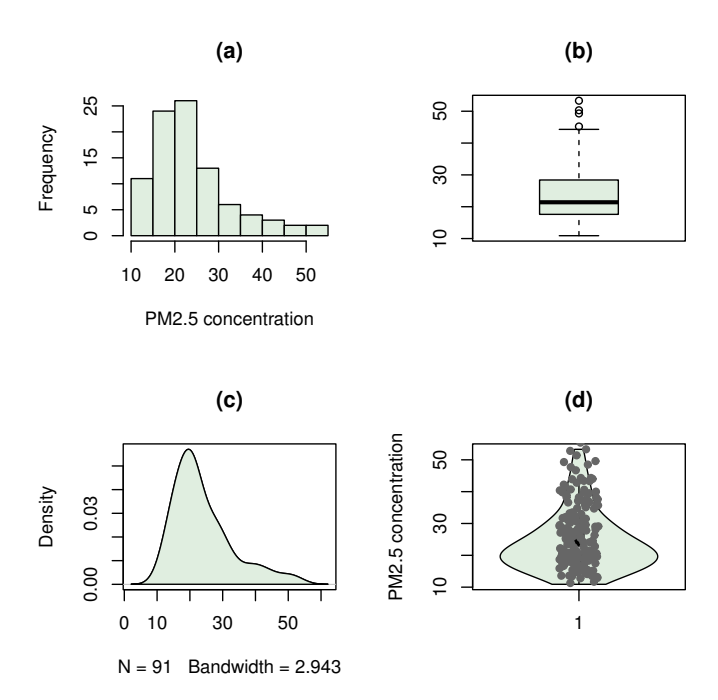


FIGURE 8. Visual representations of the PM2.5 concentration data in Phaya Thai District: (a) Histogram, (b) Box and Whisker plot, (c) Kernel density plot, and (d) Violin plot

Table 7. Comparative analysis of model fit statistics for different distributions applied to PM2.5 concentration data in Phaya Thai District

Distribution	Estimate (SE)	LogLik	AIC	BIC
XRani	0.2092 (0.0098)	-324.068	650.137	652.648
Akash	$0.1249 \ (0.0075)$	-337.135	676.269	678.780
Akshaya	$0.1606 \ (0.0084)$	-331.103	664.206	666.716
Amarendra	$0.1647 \ (0.0086)$	-329.710	661.419	663.930
Aradhana	$0.1205 \ (0.0073)$	-339.429	680.857	683.368
Sujatha	$0.1225 \ (0.0074)$	-338.374	678.749	681.260
Shanker	$0.0833 \ (0.0062)$	-350.784	703.567	706.078
Adya	$0.1247 \ (0.0075)$	-337.001	676.002	678.513
Garima	$0.0658 \ (0.0059)$	-370.578	743.156	745.667
Komal	$0.0802 \ (0.0059)$	-353.712	709.424	711.935
Ishita	$0.1254 \ (0.0076)$	-336.711	675.422	677.933
Iwok-Nwikpe	$0.1231 \ (0.0075)$	-337.943	677.886	680.397
Pratibha	$0.1230 \ (0.0074)$	-337.997	677.993	680.504
Chris-Jerry	$0.1223 \ (0.0075)$	-340.324	682.648	685.159
Lindley	$0.0833 \ (0.0062)$	-353.597	709.195	711.705
Exponential	0.0418 (0.0044)	-379.831	761.663	764.174

Note. Bold values indicate the best-fitting model based on minimum AIC and BIC values.



The KS test was applied to evaluate the suitability of the XRani distribution for modeling the PM2.5 concentration data in Phaya Thai District. The analysis produced a KS statistic of 0.1132 with a corresponding p-value of 0.1939. Given that the p-value is greater than the significant level of 0.05, the null hypothesis that the data follow the XRani distribution cannot be rejected. This result suggests that the XRani distribution is a plausible model for the observed data.

Moreover, the plotted points in the PP plot (Figure 9) exhibit a strong alignment with the diagonal reference line, indicating that the XRani distribution provides a good fit to the PM2.5 concentration data in Phaya Thai District. Although minor deviations are present at the distribution tails, the overall pattern suggests that the XRani distribution effectively captures the underlying structure of the data.

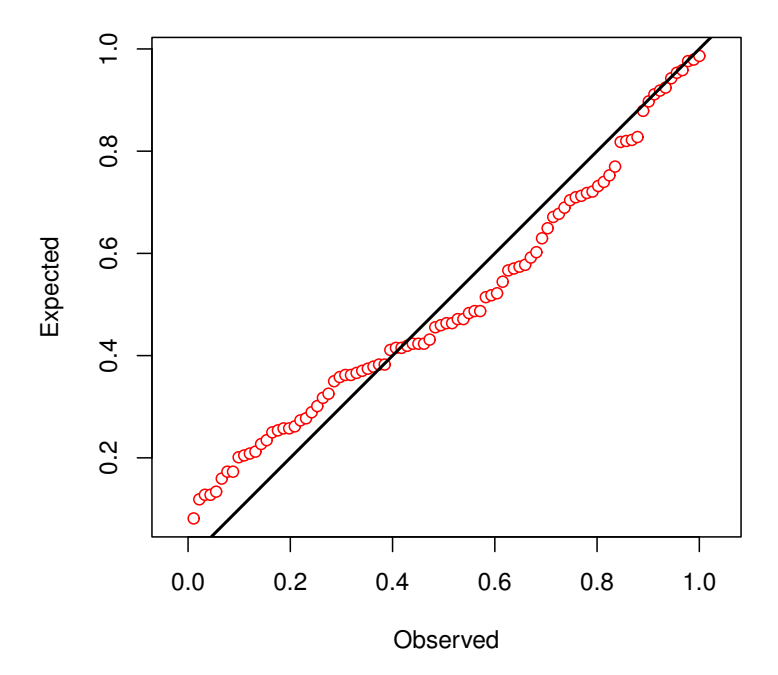


FIGURE 9. P-P plot of the PM2.5 concentration data in Phaya Thai District.

The XRani distribution demonstrated the best fit among the candidates, evidenced by its lowest AIC and BIC values. Its maximum likelihood estimate for the model parameter was 0.2092. The 95% two-sided CIs for the parameter of the XRani distribution are presented in Table 8. The CI obtained from the likelihood-based approach was (0.1905, 0.2290), corresponding to a width of 0.0385. A comparable interval was generated by the Wald-type method, spanning from 0.1890 to 0.2284, though with a slightly broader width of 0.0394. In contrast, both the bootstrap-t and BCa bootstrap approaches yielded marginally narrower intervals–(0.1935, 0.2256) and (0.1935, 0.2262), respectively.

CI Method	95% CI		99% CI		
Of Moniod	Interval	Width	Interval	Width	
Likelihood-based Wald-type Bootstrap-t BCa bootstrap	(0.1905, 0.2290) (0.1890, 0.2284) (0.1935, 0.2256) (0.1935, 0.2262)	0.0385 0.0394 0.0321 0.0327	(0.1849, 0.2355) (0.1839, 0.2344) (0.1882, 0.2317) (0.1880, 0.2317)	0.0505 0.0505 0.0435 0.0437	

Table 8. The 95% and 99% two-sided CIs and corresponding widths based on PM2.5 concentration data in Phaya Thai District

The observed performance of the CI methods in the analysis of real environmental data aligns well with the simulation findings, thus providing empirical support for the methodological conclusions drawn from the Monte Carlo study.

These findings are consistent with previous empirical studies of PM2.5 in Northern Thailand, such as those by Thangjai et al. [41] and Chankham et al. [6], which also utilized distributional methods for environmental data modeling.

Upon estimating the CI for the XRani distribution parameter, it can be easily converted into the appropriate CI for the mean PM2.5 concentration, according to the established analytical link between the parameter and the mean. This interval measures the range of credible average PM2.5 concentrations in the population, considering sampling variability. This information is crucial for environmental authorities and policymakers, since it facilitates evidence-based choices on air quality management. If the upper limit of the mean PM2.5 CI approaches or surpasses specified safety standards, it would indicate the necessity for proactive mitigation efforts, enhanced emissions regulations, or public health advisories. Narrower intervals that stay within acceptable limits can facilitate the deployment of resources to other urgent environmental concerns while ensuring continuous monitoring.

## 5. Conclusions

This paper proposed and evaluated four distinct methods for constructing two-sided confidence intervals (CIs) for the parameter of the XRani distribution: the likelihood-based, Wald-type, bootstrap-t, and bias-corrected and accelerated (BCa) bootstrap approaches. An explicit analytical expression was derived for the Wald-type CI to facilitate practical implementation. Extensive Monte Carlo simulation studies were conducted to examine the performance of these CIs under varying sample sizes and parameter values. The evaluation was based on empirical coverage probability (ECP) and average width (AW) as key performance metrics. Based on both simulation and real-world analysis, the likelihood-based and Wald-type CIs consistently demonstrated high reliability, achieving ECPs close to the nominal 0.95 level across most scenarios, especially with small to moderate sample sizes. In contrast, the bootstrap-t and BCa bootstrap methods yielded narrower intervalsindicating greater precisionbut were prone to undercoverage in small samples or under higher parameter values. However, their performance improved notably with larger sample sizes.

The practical utility of these methods was further validated using daily PM2.5 concentration data from Bang Kapi and Phaya Thai Districts in Bangkok, where the XRani



distribution demonstrated the most suitable fit among fourteen candidate distributions based on AIC and BIC. To further assess the goodness-of-fit beyond AIC and BIC, we plotted the probability probability (PP) plots for the XRani distribution. The PP plots revealed that the XRani distribution's empirical cumulative distribution function (ECDF) aligned most closely with the theoretical CDF, supporting its fit to the PM2.5 data in both Bang Kapi and Phaya Thai districts. These graphical assessments complement the information-theoretic criteria and strengthen the evidence for the XRani distributions suitability.

The CIs constructed from these real datasets aligned with the simulation findings. Overall, the likelihood-based method is recommended for applications requiring accurate coverage and computational stability, while the BCa bootstrap method may be suitable when narrower intervals are desired and sufficient data are available.

#### 6. RECOMMENDATIONS

In practice, the choice of CI method should be guided by data characteristics, computational resources, and the required level of accuracy. The likelihood-based method demonstrated consistently high coverage and moderate interval width, making it a reliable option for most applications, especially in small to moderate samples where coverage accuracy is essential. The Wald-type method, while computationally efficient and easy to implement, may underperform in skewed or heavy-tailed distributions, particularly when the sample size is small.

Bootstrap methods offer flexible alternatives. The bootstrap-t CI can be effective when standard errors are estimable, but it requires larger sample sizes to perform well. The BCa bootstrap method, which adjusts for both bias and skewness, is particularly suitable for data exhibiting asymmetry or when traditional methods show undercoverage. However, the BCa bootstrap method is computationally intensive and may require a larger number of bootstrap replications to stabilize the interval bounds. Therefore, its use is recommended when sufficient computing power and larger datasets are available.

Practitioners may prefer the likelihood-based method for its robust performance, while the BCa bootstrap method may be selected in situations where accurate quantification of uncertainty is critical and resources allow for extensive resampling.

The computational requirements of bootstrap techniques, particularly the bootstrap-t and BCa bootstrap CIs, can present challenges when working with limited computational resources. This is especially relevant in large-scale resampling or real-time applications. To support the implementation of these methods in RStudio, several robust packages are available. Among them, the 'boot' package [5] and the 'bootstrap' package [18] are widely used and provide convenient functions for constructing bootstrap confidence intervals efficiently.

The construction of accurate CIs for a distribution parameter has important implications for environmental monitoring and policy-making. For instance, in PM2.5 analysis, precise estimation of the distributional parameter enables policymakers to quantify exposure risks, set regulatory thresholds, and assess compliance with air quality standards. CIs that are too wide may indicate the need for more extensive data collection, while undercoverage could lead to misleading inferences that underestimate public health risks. By providing robust and interpret able intervalsparticularly through the likelihood-based method—this study contributes to strengthening evidence-based decision-making in urban pollution management.

# 7. Limitations

In this section, we evaluate the robustness of the CI methods to distribution misspecification. All simulation datasets are generated from an  $\varepsilon$ -contaminated distribution in which a heavy-tailed distribution serves as the contaminant. This design introduces rare but influential extremes and provides a stringent stress test for the procedures under study. In this context, robustness refers to the stability of CI procedures when the data-generating process deviates from the assumed XRani distribution.

To formalize departures from the distribution, we adopt an  $\varepsilon$ -contamination framework in which observations are drawn from a two component mixture: with probability  $1-\varepsilon$  from the target XRani distribution (the clean distribution) and with probability  $\varepsilon$  from a contaminant distribution. Heavy-tailed contamination is of particular practical interest because it generates rare but influential extremes that challenge asymptotic approximations and inflate sampling variability. We therefore use a Pareto contaminant to control both the frequency of contamination ( $\varepsilon$ ) and the severity of tail risk via its shape parameter; the contaminant scale is aligned to the XRani scale for comparability.

Let  $X \sim \text{Rani}(\theta)$ . We introduce contamination through a Pareto component  $C \sim \text{Pareto}(x_m = 1/\theta, \alpha = 1.5)$ , and form a two-component mixture

$$Y = \begin{cases} X, & \text{with probability } 1 - \varepsilon, \\ C, & \text{with probability } \varepsilon. \end{cases}$$

We fix  $\varepsilon=0.2$ . The simulation results in the case of the contaminated XRani distribution are reported in Tables 9 and 10. Under heavy-tailed contamination, none of the four CI procedures reaches the nominal 95% coverage. Coverage is uniformly poor for smallmoderate  $\theta$  (0.200.75), with BCa and bootstrap-t CIs consistently exceeding likelihood and Wald CIs yet still far below 0.95. Coverage typically decreases as n increases, reflecting CIs that become narrower around a misspecified center. For example, when  $\theta$  equals 0.30, the coverage of the BCa bootstrap CI falls from about 0.3525 at sample size 10 to about 0.1290 at sample size 500. For larger  $\theta$ , likelihood-based and Wald-type CIs may appear higher at very small n, but coverage declines most rapidly as n increases. Overall, BCa CI demonstrates the highest coverage, succeeded by bootstrap-t CI, while likelihood-based CI and Wald-type CI yield similar and somewhat lower coverage; however, all remain far below the nominal confidence level, indicating that none of them is robust when the data are contaminated by a heavy-tailed distribution.

Average width decreases with n for every interval estimation method and increases with  $\theta$  at fixed n, indicating greater inherent scale at larger  $\theta$ . Bootstrap CIs are generally wider than likelihood-based and Wald-type CIs—especially for smaller values of  $\theta$ —which corresponds with their relatively better coverage. For example, when  $\theta$  is 0.50 and the sample size is 100, the BCa bootstrap CI has coverage of about 0.3609, whereas the likelihood-based CI reaches about 0.1359. For large  $\theta$  and very small n, this pattern can be mixed, but the dominant trend remains: AWs decrease as n grows, increase with  $\theta$ , and bootstrap CIs tend to trade greater AW for comparatively higher coverage under contamination.

Table 9. Empirical coverage probability and average width of the 95% two-sided CIs for the parameter of the contaminated XRani distribution ( $\theta=0.20,\,0.30,\,0.50,\,$  and 0.75)

$\theta$	$\overline{n}$	Empirica	l Covera	ge Proba	bility	I	Average V	Width	
		Likelihood	Wald	Boot-t	BCa	Likelihood	Wald	Boot-t	BCa
0.20	10	0.1186	0.1365	0.3405	0.3770	0.2194	0.2173	0.3240	0.3432
	20	0.0868	0.0920	0.3165	0.3615	0.1430	0.1424	0.2722	0.2787
	30	0.0532	0.0565	0.2340	0.2925	0.1166	0.1162	0.2410	0.2461
	50	0.0365	0.0375	0.2150	0.2920	0.0865	0.0865	0.2120	0.2148
	100	0.0215	0.0220	0.1755	0.2590	0.0596	0.0596	0.1734	0.1750
	200	0.0140	0.0140	0.1150	0.2085	0.0415	0.0415	0.1444	0.1478
	300	0.0000	0.0000	0.0405	0.1185	0.0338	0.0332	0.1191	0.1277
	500	0.0107	0.0110	0.1215	0.2300	0.0249	0.0244	0.1196	0.1295
0.30	10	0.0991	0.1180	0.3400	0.3525	0.3168	0.3170	0.4666	0.4754
	20	0.0695	0.0760	0.2905	0.3265	0.2124	0.2125	0.3966	0.4003
	30	0.0485	0.0515	0.2415	0.2940	0.1712	0.1712	0.3569	0.3593
	50	0.0370	0.0380	0.2210	0.3035	0.1274	0.1274	0.3104	0.3110
	100	0.0190	0.0200	0.1570	0.2535	0.0891	0.0891	0.2553	0.2584
	200	0.0165	0.0165	0.0915	0.1555	0.0626	0.0626	0.2037	0.2071
	300	0.0135	0.0135	0.1125	0.2125	0.0488	0.0488	0.1897	0.1962
	500	0.0030	0.0025	0.0480	0.1290	0.0388	0.0388	0.1615	0.1669
0.50	10	0.1392	0.1515	0.3405	0.3830	0.4314	0.4331	0.6120	0.6000
	20	0.0800	0.0830	0.2750	0.3405	0.3034	0.3043	0.5373	0.5292
	30	0.0606	0.0645	0.2600	0.3250	0.2448	0.2450	0.4998	0.4950
	50	0.0410	0.0425	0.2370	0.3235	0.1894	0.1896	0.4518	0.4467
	100	0.0231	0.0230	0.1320	0.2230	0.1359	0.1352	0.3577	0.3609
	200	0.0120	0.0120	0.0930	0.1810	0.0953	0.0954	0.2933	0.2973
	300	0.0040	0.0040	0.0630	0.1215	0.0778	0.0778	0.2652	0.2715
	500	0.0010	0.0015	0.0740	0.1815	0.0594	0.0594	0.2505	0.2599
0.75	10	0.1366	0.1430	0.2605	0.3700	0.5007	0.5008	0.6038	0.6055
	20	0.0845	0.0860	0.2245	0.3375	0.3510	0.3514	0.5445	0.5470
	30	0.0665	0.0675	0.2090	0.3235	0.2894	0.2897	0.5039	0.5037
	50	0.0410	0.0415	0.1690	0.2975	0.2242	0.2244	0.4425	0.4511
	100	0.0285	0.0285	0.1335	0.2205	0.1588	0.1589	0.3767	0.3873
	200	0.0120	0.0120	0.1125	0.2260	0.1114	0.1115	0.3254	0.3462
	300	0.0035	0.0035	0.0700	0.1535	0.0923	0.0923	0.2761	0.2911
	500	0.0000	0.0000	0.0445	0.1095	0.0716	0.0716	0.2314	0.2487

Table 10. Empirical coverage probability and average width of the 95% two-sided CIs for the parameter of the contaminated XRani distribution ( $\theta = 1.00, 1.50, 2.00, \text{ and } 2.50$ )

$\overline{\theta}$	n	Empirica	l Covera	ge Proba	bility	I	Average V	Width	
		Likelihood	Wald	Boot-t	BCa	Likelihood	Wald	Boot-t	BCa
1.00	10	0.2100	0.2140	0.2660	0.3910	0.5425	0.5394	0.5793	0.5948
	20	0.1055	0.1080	0.2155	0.3555	0.3809	0.3801	0.5052	0.5188
	30	0.0805	0.0830	0.2100	0.3540	0.3084	0.3081	0.4718	0.4946
	50	0.0585	0.0600	0.1845	0.3295	0.2393	0.2392	0.4183	0.4449
	100	0.0310	0.0315	0.1510	0.2955	0.1696	0.1696	0.3475	0.3749
	200	0.0085	0.0085	0.1110	0.2280	0.1187	0.1187	0.2958	0.3220
	300	0.0130	0.0130	0.1175	0.2110	0.0961	0.0961	0.2980	0.3205
	500	0.0080	0.0080	0.0735	0.1755	0.0754	0.0754	0.2370	0.2581
1.50	10	0.7925	0.8575	0.5975	0.6975	0.6442	0.6305	0.5562	0.6131
	20	0.6525	0.6765	0.5650	0.6665	0.4402	0.4362	0.4654	0.4999
	30	0.5720	0.5955	0.5385	0.6480	0.3541	0.3522	0.4335	0.4682
	50	0.4930	0.5100	0.5440	0.6550	0.2703	0.2695	0.3670	0.4030
	100	0.3565	0.3620	0.4820	0.6160	0.1894	0.1891	0.2964	0.3267
	200	0.2535	0.2560	0.4145	0.5455	0.1334	0.1333	0.2236	0.2514
	300	0.1555	0.1585	0.3895	0.5400	0.1083	0.1082	0.2269	0.2605
	500	0.1365	0.1380	0.3265	0.4765	0.0825	0.0825	0.2237	0.2727
2.00	10	0.8760	0.8610	0.8340	0.8270	0.8701	0.8264	0.6134	0.7350
	20	0.8140	0.7920	0.8620	0.8055	0.5596	0.5476	0.5045	0.5691
	30	0.7645	0.7480	0.8475	0.7660	0.4473	0.4413	0.4443	0.4914
	50	0.6570	0.6225	0.7805	0.6415	0.3363	0.3338	0.3749	0.4128
	100	0.4070	0.3835	0.5680	0.3765	0.2314	0.2306	0.2995	0.3300
	200	0.1320	0.1200	0.2530	0.1010	0.1609	0.1606	0.2432	0.2717
	300	0.0700	0.0610	0.1515	0.0510	0.1323	0.1321	0.2070	0.2262
	500	0.0040	0.0040	0.0795	0.0030	0.1003	0.1003	0.2323	0.2492
2.50	10	0.8850	0.8375	0.7925	0.8020	1.6994	1.5974	1.1288	1.4664
	20	0.8280	0.7625	0.7665	0.7795	1.0345	0.9879	0.7774	0.9138
	30	0.7285	0.6610	0.6880	0.6925	0.7663	0.7410	0.6547	0.7530
	50	0.6220	0.5540	0.5880	0.5740	0.5679	0.5561	0.5330	0.5926
	100	0.3410	0.2835	0.3100	0.2640	0.3730	0.3693	0.4002	0.4362
	200	0.1065	0.0905	0.1005	0.0755	0.2608	0.2595	0.2993	0.3186
	300	0.0185	0.0145	0.0235	0.0140	0.2098	0.2091	0.2564	0.2715
	500	0.0040	0.0035	0.0035	0.0025	0.1635	0.1632	0.2111	0.2237

# 8. Future Work

Although this study focused on four widely used methods for constructing proposed CIs, other modern approaches such as the Bayesian CI also merit consideration. The Bayesian CI, which incorporates prior information and provides a posterior probability-based interval, may be particularly useful in settings with prior domain knowledge. While Bayesian CI was not included in the present study due to the increased computational



burden and the need for additional modeling assumptions (e.g., prior selection in Bayesian analysis), future research should explore their applicability to the XRani distribution and compare their performance in terms of ECP and AW.

Future research may explore hypothesis testing procedures and predictive modeling based on the XRani distribution, extend CI estimation methods to handle censored lifetime data, and develop Bayesian credible intervals. Moreover, investigating robust estimation techniques under model uncertainty and extending the XRani distribution framework to multivariate data settings would further enrich the statistical toolbox available for flexible and accurate inference.

#### ACKNOWLEDGEMENTS

We sincerely thank the reviewers for their valuable time and effort in reviewing our manuscript and providing insightful suggestions and recommendations. This study was supported by the Thammasat University Research Unit in Mathematical Sciences and Applications.

#### References

- [1] P. Schober, T.R. Vetter, Survival analysis and interpretation of time-to-event data: The tortoise and the hare, Anesthesia & Analgesia 127(3) (2018) 792–798. Available from: https://doi.org/10.1213/ANE.000000000003653.
- [2] O. Al-Ta'ani, M. Gharaibeh, Ola distribution: A new one parameter model with applications to engineering and COVID-19 data, Applied Mathematics & Information Sciences 17(2) (2023) 243–252. Available from: https://doi.org/10.18576/amis/170207.
- [3] F. Bittmann, Bootstrapping: An integrated approach with Python and Stata, Munich: De Gruyter Oldenbourg (2021). Available from: https://doi.org/10.1515/9783110693348.
- [4] S.P. Brooks, A. Gelman, General methods for monitoring convergence of iterative simulations, Journal of Computational and Graphical Statistics 7(4) (1998) 434–455. Available from: https://doi.org/10.1080/10618600.1998.10474787.
- [5] A. Canty, B. Ripley, Package boot. Bootstrap functions (2024). Available from: https://cran.r-project.org/package=boot.
- [6] W. Chankham, S.A. Niwitpong, S. Niwitpong, The simultaneous confidence interval for the ratios of the coefficients of variation of multiple inverse Gaussian distributions and its application to PM2.5 data, Symmetry 16(3) (2024) 331. Available from: https://doi.org/10.3390/sym16030331.
- [7] G.W. Corder, D.I. Foreman, Nonparametric statistics: A step-by-step approach. Hoboken: John Wiley & Sons (2014).
- [8] A.C. Davison, D.V. Hinkley, Bootstrap methods and their application. Santa Barbara: Cambridge University Press (1997).
- [9] U.V. Echebiri, J.I. Mbegbu, Juchez probability distribution: Properties and applications, Asian Journal of Probability and Statistics 20(2) (2022) 56–71. Available from: https://doi.org/10.9734/ajpas/2022/v20i2419.
- [10] O. Elechi, E. Okereke, I. Chukwudi, K. Chizoba, O. Wale, Iwueze's distribution and its application, Journal of Applied Mathematics and Physics 10(12) (2022) 3783–3803. Available from: https://doi.org/10.4236/jamp.2022.1012251.

- [11] H.O. Etaga, C.K. Onyekwere, D.O. Oramulu, O.J. Obulezi, A new modification of Rani distribution with more flexibility in application, Scholars Journal of Physics, Mathematics and Statistics 10(7) (2023) 160–176. Available from: https://doi.org/10.36347/sjpms.2022.v10i07.003.
- [12] A. Gelman, J.B. Carlin, H.S. Stern, D.B. Dunson, A. Vehtari, D.B. Rubin, Bayesian data analysis. Boca Raton: CRC Press (2013).
- [13] M. Gharaibeh, Gharaibeh distribution and its applications, Journal of Statistics Applications & Probability 10(2) (2021) 441–452. Available from: https://doi.org/10.18576/jsap/100214.
- [14] M. Ghitany, B. Atieh, S. Nadarajah, Lindley distribution and its applications, Mathematics and Computers in Simulation 78(4) (2008) 493–506. Available from: https://doi.org/10.1016/j.matcom.2007.06.007.
- [15] A. Henningsen, O. Toomet, MaxLik: A package for maximum likelihood estimation in R, Computational Statistics 26 (2011) 443–458. Available from: https://doi.org/10.1007/s00180-010-0217-1.
- [16] I.A. Iwok, B.J. Nwikpe, The Iwok-Nwikpe distribution: Statistical properties and its application, Asian Journal of Probability and Statistics 15(1) (2021) 35–45. Available from: https://doi.org/10.9734/ajpas/2021/v15i130347.
- [17] J. Kiusalaas, Numerical methods in engineering with Python 3. Cambridge: Cambridge University Press (2013).
- [18] S. Kostyshak, Package bootstrap. Functions for the book "An introduction to the bootstrap" (2024). Available from: https://cran.r-project.org/web/packages/bootstrap.
- [19] E.T. Lee, J.W. Wang, Statistical methods for survival data analysis. New York: John Wiley & Sons (2003).
- [20] A.A. Nanvapisheh, S.M.T.K. MirMostafaee, E. Altun, A new two-parameter distribution: Properties and applications, Journal of Mathematical Modeling 7(1) (2019) 35–48. Available from: https://doi.org/10.22124/jmm.2018.9994.1148.
- [21] A.W. Nwry, H.M. Kareem, R.B. Ibrahim, S.M. Mohammed, Comparison between bisection, Newton, and secant methods for determining the root of the non-linear equation using MATLAB, Turkish Journal of Computer and Mathematics Education 12(14) (2021) 1115–1122. Available from: https://doi.org/10.17762/turcomat.v12i14.10397.
- [22] O.B. Olufemi-Ojo, S.I. Onyeagu, H.O. Obiora Ilouno, On the application of two-parameter Shanker distribution, International Journal of Innovative Science and Research Technology 9(1) (2024) 807–820. Available from: https://doi.org/10.5281/zenodo.10559198.
- [23] C. Onyekwere, O. Obulezi, Chris-Jerry distribution and its applications, Asian Journal of Probability and Statistics, 20, 16–30. (2022). Available from: https://doi.org/10.9734/AJPAS/2022/v20i130480.
- [24] Y. Pawitan, In all likelihood: Statistical modeling and inference using likelihood. Oxford: Clarendon Press (2001).
- [25] C.P. Robert, G. Casella, Monte Carlo statistical methods. New York: Springer (2004).
- [26] T.A. Severini, Likelihood methods in statistics. Oxford: Oxford University Press (2000).



- [27] R. Shanker, S. Sharma, R. Shanker, A two-parameter Lindley distribution for modeling waiting and survival times data, Applied Mathematics 4(2) (2013) 363–368. Available from: https://doi.org/10.4236/am.2013.42056.
- [28] R. Shanker, Shanker distribution and its applications, International Journal of Statistics and Applications 5(6) (2015) 338–348. Available from: https://doi.org/10.5923/j.statistics.20150506.08.
- [29] R. Shanker, Akash distribution and its applications, International Journal of Probability and Statistics 4(3) (2015b) 65–75. Available from: https://doi.org/10.5923/j.ijps.20150403.01.
- [30] R. Shanker, Aradhana distribution and its applications, International Journal of Statistics and Applications 6(1) (2016) 23–34. Available from: https://doi.org/10.5923/j.statistics.20160601.04.
- [31] R. Shanker, Amarendra distribution and its applications, American Journal of Mathematics and Statistics 6(1) (2016) 44–56. Available from: https://doi.org/10.5923/j.ajms.20160601.05.
- [32] R. Shanker, Sujatha distribution and its applications, Statistics in Transition. New Series 17 (2016) 391–410. Available from: https://doi.org/10.21307/stattrans-2016-029.
- [33] R. Shanker, Garima distribution and its application to model behavioral science data, Biometrics & Biostatistics International Journal 4(7) (2016) 275–281. Available from: https://doi.org/10.15406/bbij.2016.04.00116.
- [34] R. Shanker, Rani distribution and its application, Biometrics & Biostatistics International Journal 6(1) (2017) 256–265. Available from: https://doi.org/10.15406/bbij.2017.06.00155.
- [35] R. Shanker, Akshaya distribution and its application, American Journal of Mathematics and Statistics 7(2) (2017) 51–59. Available from: https://doi.org/10.5923/j.ajms.20170702.01.
- [36] R. Shanker, K.K. Shukla, Ishita distribution and its applications, Biometrics & Biostatistics International Journal 5(2) (2017) 39–46. Available from: https://doi.org/10.15406/bbij.2017.05.00126.
- [37] R. Shanker, K.K. Shukla, R. Shanker, T.A. Leonida, A three-parameter Lindley distribution, American Journal of Mathematics and Statistics 7(1) (2017) 15–26. Available from: https://doi.org/10.5923/j.ajms.20170701.03.
- [38] R. Shanker, Komal distribution with properties and application in survival analysis, Biometrics & Biostatistics International Journal 12(2) (2023) 40–44. Available from: https://doi.org/10.15406/bbij.2023.12.00381.
- [39] R. Shanker, Pratibha distribution with properties and application, Biometrics & Biostatistics International Journal 13 (2023) 136–142. Available from: https://doi.org/10.15406/bbij.2023.12.00397.
- [40] R. Shanker, K. Shukla, Adya distribution with properties and application, Biometrics & Biostatistics International Journal 10 (2021) 81–88. Available from: https://doi.org/10.15406/bbij.2021.10.00334.
- [41] W. Thangjai, S. Niwitpong, S. Niwitpong, Estimation of the percentile of Birnbaum-Saunders distribution and its application to PM2.5 in Northern Thailand. PeerJ 12 (2024) e17019. Available from: https://doi.org/10.7717/peerj.17019.